

Article

Quantitative EEG Markers of Entropy and Auto Mutual Information in Relation to MMSE Scores of Probable Alzheimer's Disease Patients

Carmina Coronel ^{1,*}, Heinrich Garn ¹, Markus Waser ¹, Manfred Deistler ², Thomas Benke ³, Peter Dal-Bianco ⁴, Gerhard Ransmayr ⁵, Stephan Seiler ⁶, Dieter Grossegger ⁷ and Reinhold Schmidt ⁶

¹ AIT Austrian Institute of Technology GmbH, 1220 Vienna, Austria; heinrich.garn@ait.ac.at (H.G.); markus.waser@ait.ac.at (M.W.)

² Institute of Statistics and Mathematical Methods in Economics, Vienna University of Technology, 1040 Vienna, Austria; manfred.deistler@tuwien.ac.at

³ Clinic of Neurology, Medical University of Innsbruck, 6020 Innsbruck, Austria; thomas.benke@i-med.ac.at

⁴ Department of Clinical Neurology, Medical University of Vienna, 1090 Vienna, Austria; peter.dal-bianco@meduniwien.ac.at

⁵ Department of Neurology 2, MedCampus III of the Kepler University Hospital, 4021 Linz, Austria; gerhard.ransmayr@keplerunivklinikum.at

⁶ Department of Neurology, Clinical Division of Neurogeriatrics, Medical University of Graz, 8036 Graz, Austria; stephan.seiler@medunigraz.at (S.S.); reinhold.schmidt@medunigraz.at (R.S.)

⁷ Dr. Grossegger & Drbal GmbH, Ruthgasse 19, 1190 Vienna, Austria; office@alphatrace.at

* Correspondence: carmina.coronel@ait.ac.at; Tel.: +43-505-504-155

Academic Editor: Osvaldo Anibal Rosso

Received: 17 December 2016; Accepted: 3 March 2017; Published: 17 March 2017

Abstract: Analysis of nonlinear quantitative EEG (qEEG) markers describing complexity of signal in relation to severity of Alzheimer's disease (AD) was the focal point of this study. In this study, 79 patients diagnosed with probable AD were recruited from the multi-centric Prospective Dementia Database Austria (PRODEM). EEG recordings were done with the subjects seated in an upright position in a resting state with their eyes closed. Models of linear regressions explaining disease severity, expressed in Mini Mental State Examination (MMSE) scores, were analyzed by the nonlinear qEEG markers of auto mutual information (AMI), Shannon entropy (ShE), Tsallis entropy (TsE), multiscale entropy (MsE), or spectral entropy (SpE), with age, duration of illness, and years of education as co-predictors. Linear regression models with AMI were significant for all electrode sites and clusters, where R^2 is 0.46 at the electrode site C3, 0.43 at Cz, F3, and central region, and 0.42 at the left region. MsE also had significant models at C3 with $R^2 > 0.40$ at scales $\tau = 5$ and $\tau = 6$. ShE and TsE also have significant models at T7 and F7 with $R^2 > 0.30$. Reductions in complexity, calculated by AMI, SpE, and MsE, were observed as the MMSE score decreased.

Keywords: Shannon entropy; Tsallis entropy; multiscale entropy; spectral entropy; auto mutual information; Alzheimer's disease; Mini-Mental State Examination; EEG

1. Introduction

Alzheimer's disease (AD) is the leading cause of dementia [1], with the World Alzheimer Report of 2015 [2] estimating 9.9 million new dementia cases every year worldwide. AD is characterized by loss of neuronal cells and development of neurofibrillary tangles and cortical amyloid plaques [3]. It continues to be difficult to diagnose as it shares symptoms with other dementia-related diseases. Diagnosis of AD is either possible or probable [4]. Common routine diagnostic procedures and

workout for AD patients include clinical interviews with neuropsychological tests that evaluate possible cognitive deficits, imaging techniques such as structural and functional magnetic resonance imaging (MRI), and PET scans. MRI is widely available, but can be costly and is not suitable for patients who are claustrophobic, while PET scans are expensive, not easily available, and invasive, with intravenous access and exposure to radiation [5]. Use of an electroencephalogram as an aid for physicians for the diagnosis of AD is a viable option as it is widely available in neurological clinics, relatively inexpensive, noninvasive, and has mobility potential [6].

Three major effects of cognitive decline have been observed in the EEGs of AD patients: slowing of the EEG in terms of a shift in the power spectrum to lower frequencies, reduced complexity of EEG signals, and reduced coherence of signals measured at different locations on the cortex [7,8]. Furthermore, [7] pointed out the loss of connectivity in cortex of AD patients and that EEG signals are generated by nonlinear interactions between neurons. The loss of connectivity in the brain could mean deficiency in the information processing of the cortex. As such, we expect a change in the nonlinear qEEG markers describing complexity of a signal such as entropy and auto mutual information (AMI) in AD patients. The behavior of entropy and AMI in AD patients has been assessed in the past. A previous study by Jeong et al. on AMI found that the rate of decrease of AMI was correlated with MMSE scores [9]. In their investigation of multiscale entropy (MsE), Yang et al. observed a decrease in MsE complexity in short time scales in AD patients with increased severity and increased MsE complexity in long time scales [10]. On the other hand, Escudero et al. found better MsE in deeper scales of EEG in their study on AD patients and found less complexity in AD patients than in control subjects [11]. Mizuno et al. observed less complexity in the AD groups at smaller scales in the frontal area and higher complexity at larger scales was seen across the brain and was correlated with cognitive decline [12]. In their investigation of spectral entropy (SpE), 79.2% accuracy in classifying amnestic mild cognitive decline patients, AD patients and normal controls using regional SpE and complexity features was achieved by McBride et al [13]. Garn et al observed association of AMI, Shannon entropy (ShE) and Tsallis entropy (TsE) to MMSE [14,15].

While most of the previous studies have looked into the comparison of qEEG markers between AD to healthy controls or to mild cognitive impairment, the focus of this paper was to observe changes in the qEEG markers in comparison to MMSE scores at mild and moderate stages of the disease. Mini-mental state examination (MMSE) [16] is a method to evaluate the cognitive state of AD patients and have been routinely used in clinical settings. We are interested in the behavior of the markers, entropy, and AMI, at specific electrode sites or regions of the brain, as the cognitive decline of probable AD patients becomes more severe. Garn et al. [14] have shown correlation between the MMSE scores of AD patients to AMI, ShE, and TsE. Following up on the previous findings of their paper about the correlation between AD severity, as expressed by the MMSE, and the EEG markers of AMI, ShE, and TsE, the addition of other entropy definitions of SpE and MsE were examined in this paper. The same subjects from [14] participated in this study. While 79 subjects were reported in the previous paper, the eventual number of participants was effectively 64 subjects due to the automatic exclusion of data in the statistical analysis as there was missing/unknown demographic information.

The objective of this study is to investigate whether disease severity, ranging from mild to moderate, could be explained by nonlinear EEG markers, in the hope to find specific markers that could aid in the diagnosis of AD patients. No healthy controls were used in this study as the focus is on the severity of the disease in relation to the markers within probable AD patients.

2. Materials and Methods

2.1. Subjects

The 79 subjects participated in this study where all were diagnosed with probable Alzheimer's disease according to NINCDS-ADRDA criteria [4,17] (See Appendix A). All subjects were participants in the Prospective Dementia Database Austria (PRODEM), a multi-cohort study of patients diagnosed

with AD. Written consent forms were obtained from all participating subjects and their caregivers. The responsible ethics commissions approved the study.

During assessment, MMSE tests and EEG recordings were performed on all patients. As seen in Table 1, a median of 22 for MMSE was calculated. Ranging from 15 to 26 MMSE scores, all 79 probable AD patients were in the mild to moderate case. The median age of the subjects was 75, median education in years was 11, and the median duration of illness in months was 23. Distribution of age, years of education, duration of illness, and MMSE scores were illustrated in Figure 1. Fifty of the subjects were female and 29 were male. 57% percent of the patients had arterial hypertension while almost 13% of patients were diagnosed with diabetes mellitus, 10% had coronary heart disease, and 29 patients had hypercholesterolemia (See Table 1).

Table 1. Demographic information and risk factors of 79 probable Alzheimer's disease (AD) subjects.

	Range	Mean	Median	Median Absolute Deviation
<i>Demographic information</i>				
Age (years)	52–88	73.5	75	6
Education (years)	7–20	11	11	2
Duration of illness (months)	2–120	25.5	23	13
Sex (m/f)	29m/50f			
<i>Neuropsychological information</i>				
MMSE	15–26	22	22	2
<i>Risk Factors</i>				
	Yes	No	Unknown	
Arterial hypertension	45	32	2	
Diabetes mellitus	10	68	1	
Coronary heart disease	8	69	2	
Atrial fibrillation	5	71	3	
Hypercholesterolemia	29	46	4	
	Never	Earlier	Currently	Unknown
Nicotine	60	14	2	3
Alcohol	52	6	18	3

2.2. Ethical Statement

The ethics committees of the Medical University of Graz (19-135 ex 07/08), Medical University of Innsbruck (UN3259), Medical University of Vienna (176/2008) and Ethics Committee of the State of Upper Austria have approved this study.

2.3. EEG Recordings

All patients underwent EEG recordings in an upright seated position in a resting state with their eyes closed for approximately three minutes. A series of other positions and tests prescribed by physicians were also recorded. However, these took place after the three minutes of rest and were not included in this study.

Nineteen monopolar electrode sites according to the International 10/20 System were used to collect the following EEG data: Fp1, Fp2, Fz, F3, F4, F7, F8, T7, T8, Cz, C3, C4, Pz, P3, P4, P7, P8, O1, and O2. Two electrodes placed at the outer corner of the right and left eye recorded data for the horizontal electro-oculogram (HEOG). Vertical electro-oculogram (VEOG) electrodes were placed above and below the left eye. A ground electrode was placed at FCz and connected mastoid electrodes were used as references. Contact impedances were kept below 10 kΩ each. Data was collected using the AlphaEEG amplifier with NeuroSpeed software (alpha trace medical systems, Vienna, Austria). The EEG amplifier had a band pass of 0.3 to 70 Hz with a 50 Hz notch filter. Data were collected

at 256 Hz with 16 bit resolution. ECG signals were also recorded via clamp electrodes around the subjects' wrists.

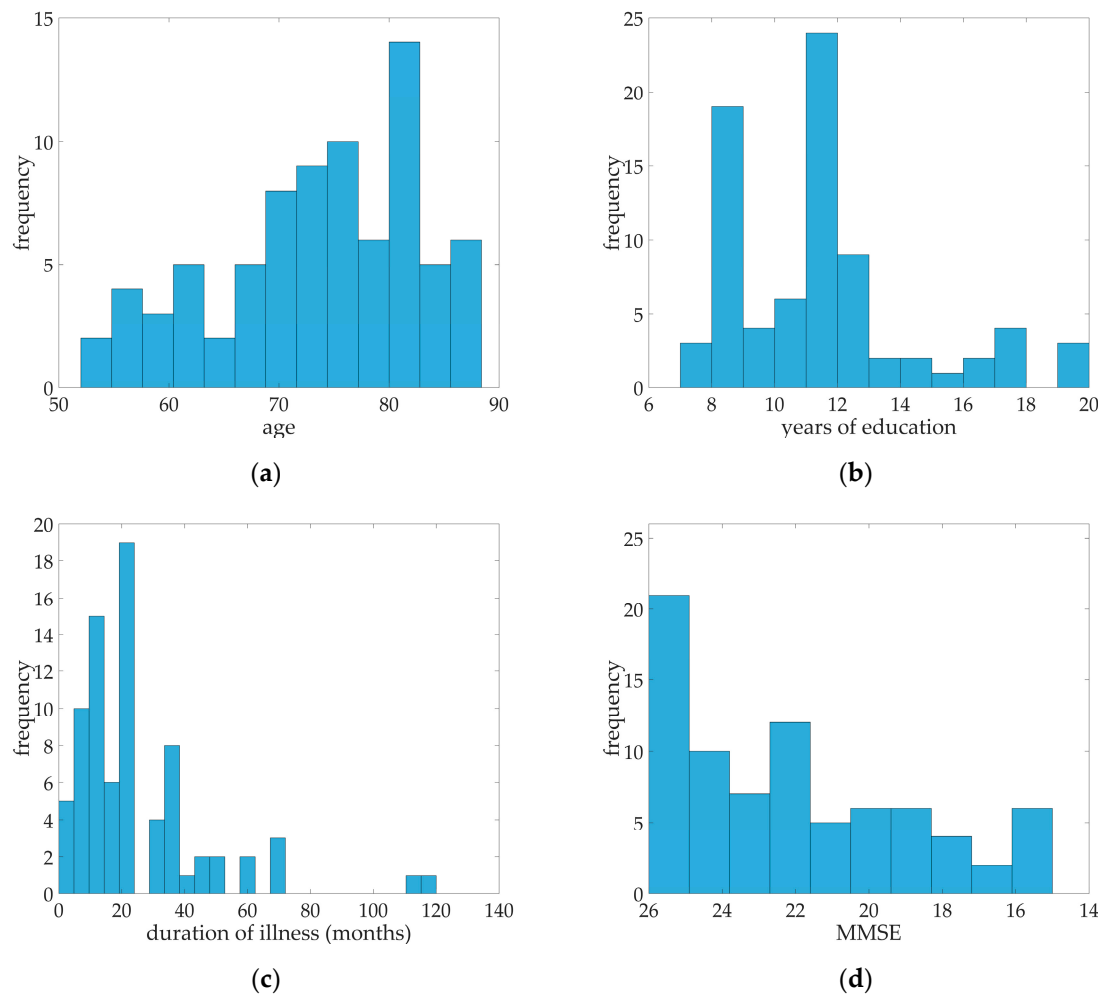


Figure 1. Histograms of (a) age; (b) years of education; (c) duration of illness; and (d) MMSE scores of the 79 subjects participating in this study.

2.4. EEG Preprocessing

All EEG recordings were preprocessed to remove any artefacts, movements, irregular segments in the recording due to loose or detached electrodes, and cardiac activity. The following steps were taken:

1. Visual inspection by an expert to exclude segments in the recording with highly irregular signals due to any patient movements, loose, or detached electrodes. An average of 168s from the total three-minute recording of the EEG was selected.
2. A 2 Hz high-pass filter was applied to all remaining EEG, EOG, and ECG signals.
3. Any interference due to eye movements, including blinking, was filtered from the EEG signal by linear regression using the HEOG and VEOG according to the Draper and Smith method [18].
4. Some EEG signals contained interference from heart signals appearing as small voltage peaks. These were removed based on the ECG signals recorded; the procedure was carried out according to a modified Pan-Tompkins algorithm and linear regression [19].

2.5. EEG Epochs

In the 3-min EEG recordings, 168 s of recording was the averaged selected EEG recordings for all 79 patients. 69 of the patients did not have segments in the EEG recordings that were excluded. The EEG markers to be obtained from the EEG recordings rely on the stationarity of the segment while the EEG signals are basically non-stationary [20]. To overcome this problem, a solution of using “quasi-stationary” segments was used for EEG markers computation. The selected EEG signals were divided into 4-s epochs with 2 s of overlap. The length of the segment was verified by the augmented Dickey-Fuller test [21]. As each patient had different number of epochs to be used, a limit of 40 epochs per patient, equivalent to 85 s, was imposed. For uniformity, only the first 40 epochs of each patient were used to calculate the EEG markers. All epoch values are provided in the supplementary materials.

2.6. qEEG Markers and Computation

This study focused on the following nonlinear qEEG markers explaining complexity of the brain signals: ShE, TsE, MsE, SpE, and AMI. Each marker was the average computed value on “quasi-stationary” 4-second segments of EEG signal for all channels or clusters. All markers were calculated in the frequency range of 2–30 Hz.

Entropy measures the predictability of a random variable, in this case, an EEG signal of channel i , as a measure of the signal’s complexity. ShE of signal $X_i = (X_i(0), \dots, X_i(t-1))$ of length T is

$$-\sum_{X_i} p(X_i) \log_2 [p(X_i)] \quad (1)$$

while TsE is calculated by

$$\frac{1}{q-1} \left(1 - \sum_{X_i} p^q(X_i) \right) \quad (2)$$

where $q \in R$ is the entropy index and is set at $q = 0.5$ for this study [14].

SpE measures the complexity of the signal not in the time domain but in the frequency domain. The power spectral density (PSD) of the signal was estimated using the Welch method. Computation of the probability density function (PDF) was carried out by the normalization of the PSD. SpE is then calculated using the ShE equation on the PDF [22].

On the other hand, MsE measures the complexity of the signal by looking at the scale of the signal. The concept of multiple scales was explained by Costa et al. [23]. The scaled signal is achieved via resampling of the original signal where a scale of $\tau = 1$ represents the original signal and increasing the τ will give a coarse-grained version of a signal. A τ scaled version of a signal $X_i^1 = (X_i(0), \dots, X_i(t-1))$ is given by

$$x_i^\tau = \frac{1}{\tau} \sum_{j=(i-1)\tau+1}^{i\tau} x_j^1 \quad (3)$$

and the MsE is achieved by computing the sample entropy of the scaled signal. For this study, $t = 2, 3, \dots, 7$ was tested. As the scale increases, the length of the scaled signal decreases, a modified version of the MsE (further referred to as MsE modified) performed by Wu et al. [24]. Their method involved replacing the scaled version of the signal by a template vector calculated by moving-average and time delay to give better estimates of the MsE. MsE and MsE modified computations were employed in this study. Computation of MsE modified in higher scales were carried out for $t = 9, 11, 13, \dots, 15$.

Mutual information (MI) is a measure of the dependence between two signals of two random variables, where a value of 0 means that two variables are independent of each other [25]. In the case of this study, the MI is measured between an EEG signal from channel i and its time-shifted version, hence it is called AMI. It is different from cross MI where it measures the dependence between two

signals [9]. AMI is the EEG marker that was investigated here. It measures the predictability of the signal, or how the original signal can predict its time-shifted version. Given that an EEG signal of channel i is $X_i = (X_i(0), \dots, X_i(t-1))$ and its time-shifted version $Y_i = (Y_1, \dots, Y_i(t-1+s))$, both with length of T , the AMI is then defined as

$$\sum_{Y_i} \sum_{X_i} p(X_i, Y_i) \log \left[\frac{p(X_i, Y_i)}{p(X_i)p(Y_i)} \right] \quad (4)$$

where $p(X_i)$, $p(Y_i)$, and $p(X_i, Y_i)$ are the estimated probability functions. A signal with higher values denotes better predictability. The AMI was calculated on individual electrode sites and on clusters defined by the regions of the brain: anterior, anterior/temporal, central, posterior, posterior/temporal, temporal-left, temporal-right, left, right, and all (See Appendix B).

2.7. Statistical Analysis

Multiple regression models were used to analyze disease severity quantified by MMSE in relation to each EEG markers per electrode site or cluster. The dependent variable was the MMSE score and the main independent variable was the specific qEEG marker, with age, duration of illness, and years of education as other predictors. The qEEG marker was added to the model as linear or in linear and squared terms. Inclusion of the other predictors was necessary as MMSE scores are affected by age and education [26]. The significance of the regression models was assessed by the Fisher's f -test. The coefficients of determination, R^2 , were compared to analyze the goodness of fit of the model. Holm-Bonferroni method [27] was used to control the familywise error rate. Given a total of 875 total statistical tests, all statistical results were ranked and sequentially tested for significance following the said method. Stability of the markers was assessed by the calculated variance of the markers per patient, given that the markers are the mean values of the calculated marker from the 40 epochs. Assessment of the individual variables of the model was based on the t -stat test, $p < 0.05$. Standardized regression coefficients were also computed to compare the coefficients of variables given the differences in the variables' units.

3. Results

Multiple regression models with significant results are shown in Tables 2 and 3. MMSE served as the dependent variable while the predictors are the qEEG markers, age, duration of illness, and years of education. The regression models with qEEG markers were expressed in linear and squared terms. All following models mentioned with significant results were tested according to the Holm-Bonferroni method. Two electrode sites resulted in significant linear regression models with ShE as the independent variable at electrodes T7 and F7 where the regression models achieved R^2 as high as 0.32 (See Figure 2) and 0.30 respectively. With a low variance for the marker ShE, where the highest is at 0.0042, it is evident that the marker remained stable across the calculation for 40 epochs per patient. The marker TsE also has a low variance (highest at 0.0075), indicating stability across the recording. Models with TsE resulted in significant results at two electrode sites, T7 and F7. The regression model performed at electrode T7 achieved $R^2 = 0.37$ (See Figure 2) while at electrode F7 the model had R^2 of 0.33. The regression models with SpE as independent variable were significant at electrodes located in the frontal, central, and temporal regions. While regression models at C3, T7, and F3 have $R^2 > 0.30$, the variance of SpE is higher (reaching up to 0.15) than that of ShE and TsE.

Table 2. Significant linear regression models results. qEEG markers expressed in linear terms only.

qEEG Markers	Electrode Sites/Clusters Where Model Is Significant According to Holm-Bonferroni Method	Highest R ²	Max Variance ^a
ShE	T7 and F7	T7: 0.32	0.0042
		F7: 0.30	0.0075
TsE	T7 and F7	T7: 0.37	0.0075
		F7: 0.33	0.0102
SpE	C3, T7, F3, Cz, Fz, C4, Fp1, F7, F4	C3: 0.33	0.1162
		T7: 0.32	0.1531
		F3: 0.31	0.1023
MsE			
$\tau = 3$	Cz, C3, Fz, F3, F4, F7, C4, T7, Pz, Fp1, F8	Cz: 0.38	0.0466
$\tau = 5$	All except P8, P7, P3, Fp2, F8, O2, T8, & O1	C3: 0.39	0.1654
MsE modified			
$\tau = 3$	C3, Cz, Fz, F3, F4, C4, F7, Pz, T7, Fp1, F8, P3	C3: 0.37	0.0490
$\tau = 5$	All except Fp2, T8, O2, & O1	C3: 0.42	0.0325
$\tau = 7$	All except T8, Fp2, O2, & O1	C3: 0.40	0.0364
$\tau = 9$	All except O1	T7: 0.37 C3: 0.36	0.0374 0.0393
$\tau = 10$	All	C3: 0.39	0.0323
$\tau = 11$	All	C3: 0.39	0.0274
$\tau = 13$	All except Fp2 & O1	C3: 0.37	0.0220
$\tau = 15$	All except Fp2	C3: 0.38	0.0234
AMI	All electrode sites except T7 & T8	C3: 0.46	0.0029
		central: 0.43 left: 0.42 all: 0.42	0.0028 0.0024 0.0020

^a Maximum calculated variances of the calculated qEEG marker from all patients. (Maximum from the set of variances calculated from the 40 epochs calculated per patient).

Table 3. Best regression models results based on *p* and R² at specific electrode sites or clusters.

qEEG Markers	Electrode Sites	R ²	<i>p</i> ($\times 10^{-4}$)	qEEG Marker ^a <i>t</i> -Stat <i>p</i> ($\times 10^{-2}$)	Significant Co-Predictors ^b
ShE	T7	0.32	0.079	0.007	A, D, E
	F7	0.30	0.215	0.021	A, D, E
TsE	T7	0.37	0.005	0.000	A, D, E
	F7	0.33	0.043	0.004	A, D, E
SpE	T7	0.32	0.082	0.007	A, D, E
MsE mod. $\tau = 5$	C3	0.42	0.000	0.000	A, D, E
MsE mod. $\tau = 6$	C3	0.41	0.000	0.000	A, D, E
AMI	C3	0.46	0.000	0.000	A, D, E
	Cz	0.43	0.000	0.000	E
	F3	0.43	0.000	0.000	A, E
	central	0.43	0.000	0.000	E
	left	0.42	0.000	0.000	A, E

^a qEEG marker as the main predictor of interest. *p* < 0.05 denotes significance; ^b Predictors other than the qEEG marker with tstat *p* < 0.05 A: age; D: duration of illness (months); E: years of education.

Age, duration of illness and years of education were significant variables for the models in Table 3 for ShE and TsE. Comparing standardized regression coefficients verified that ShE and TsE for models specified in Table 3 were the most significant variables. Adding the squared terms of the EEG markers produced quadratic regression models. ShE at T7 with linear and squared terms present in the model

does not provide a better model than having only the linear term of ShE in the model. The same was evident for TsE and SpE.

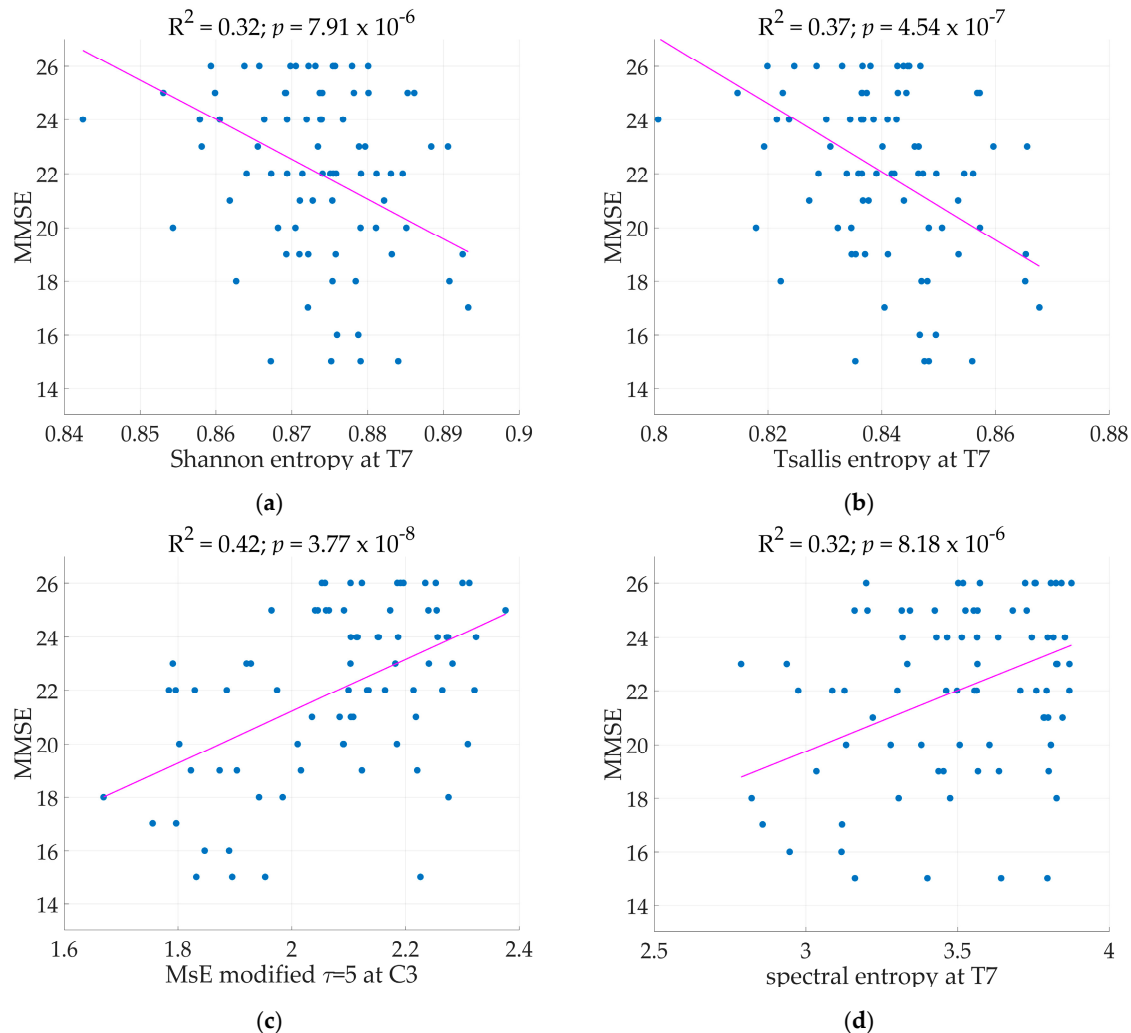


Figure 2. qEEG markers at electrode site T7 or C3. The regression lines are represented by setting co-predictors (age, duration of illness, and years of education) at mean, tabulated in Table 1. (a) ShE at T7, (b) TsE at T7, (c) MsE modified at $\tau = 5$, & (d) SpE at T7.

Across the region of the brain, all electrode sites, except T7 and T8, and clusters achieved significant regression models with AMI as the main predictor achieving R^2 as high as 0.46 at electrode C3 (Illustrated in Figure 3). Next to C3, electrode Cz and F3 achieved R^2 of 0.43 for both. Comparisons of standard regression coefficients showed AMI as the main significant predictor of the models. As expected, adding another term to the regression models increased R^2 , in this case the squared term of the qEEG markers. However, adding the squared term of the qEEG markers did not automatically constitute a better model. So was the case for AMI. As seen in Figure 4, electrodes by the perimeter resulted to lower R^2 than the electrodes situated more centrally.

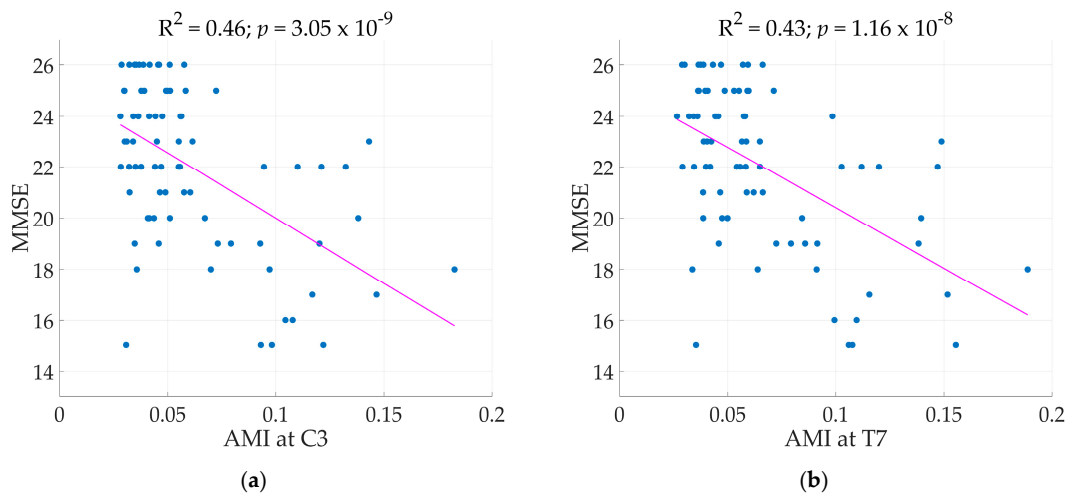


Figure 3. (a) AMI at C3 and (b) central cluster versus MMSE scores. The regression lines of models are represented by setting co-predictors (age, duration of illness, and years of education) at mean, tabulated in Table 1.

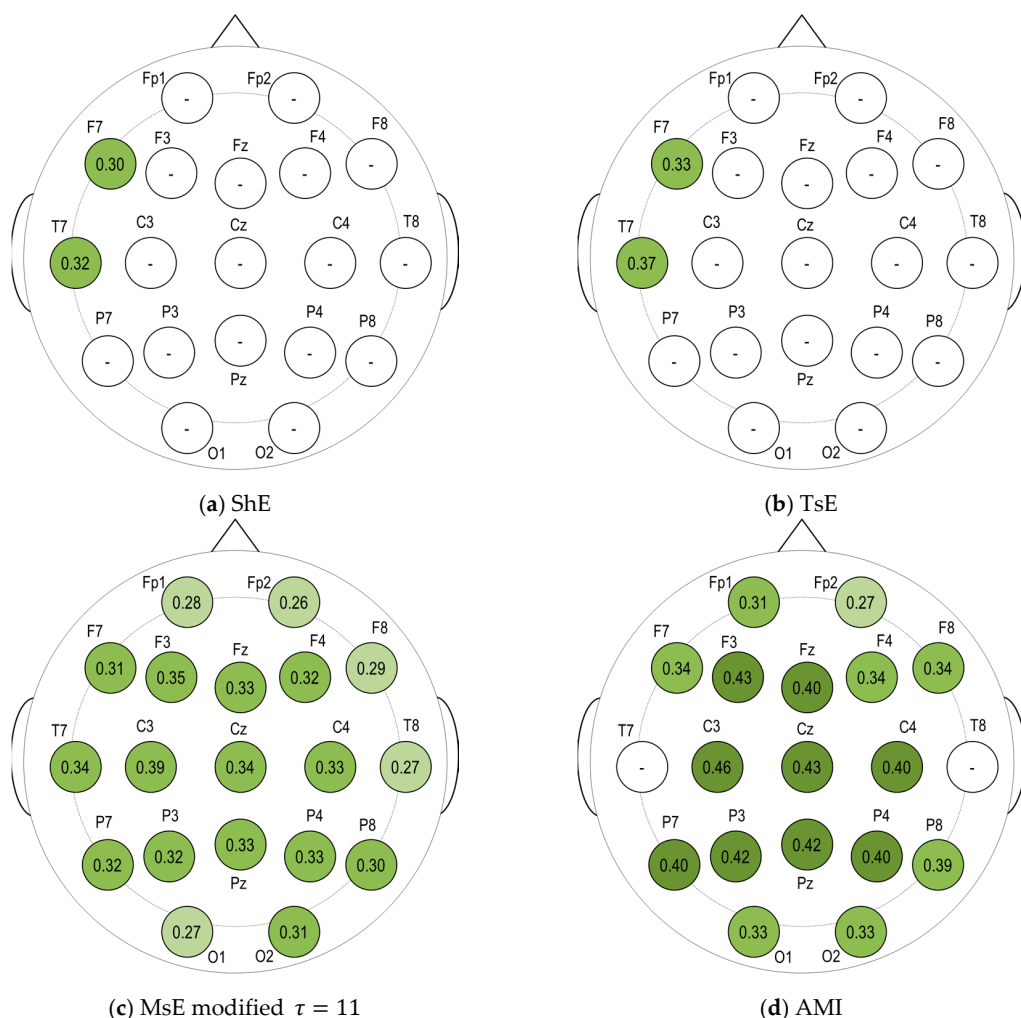


Figure 4. The computed R^2 of significant linear regression models (a) ShE, (b) TsE, (c) MsE modified $\tau = 11$, & (d) AMI at specific electrode, insignificant models are left blank. Electrode sites with $R^2 > 0.20$ are shaded in light green, $R^2 > 0.30$ in green, and $R^2 > 0.40$ in dark green.

The drawback in computing MsE at higher scales was evident in Table 2 where the variance increased dramatically at scale $\tau = 5$. The MsE modified proved to be better for all scales used in this study thus MsE modified was the only one to be discussed further. At lower scales, only 12 electrode sites resulted to significant regression models. By $\tau = 10$, all electrode sites resulted to significant regression models (Figure 4). There are electrode sites that did not exhibit significant models at lower scales, particularly at electrode O2 where significant results were only observed starting at scale $\tau = 8$, electrode Fp2 at scale $\tau = 9$, and electrode O1 at $\tau = 10$. Increasing R^2 was observed in models starting at scale $\tau = 2$ at electrode C3 and T7 reaching the maximum R^2 at $\tau = 6$ and $\tau = 9$ respectively. R^2 at other electrode sites also increased with increasing scale with varying scale where it reached the maximum (Figure 5).

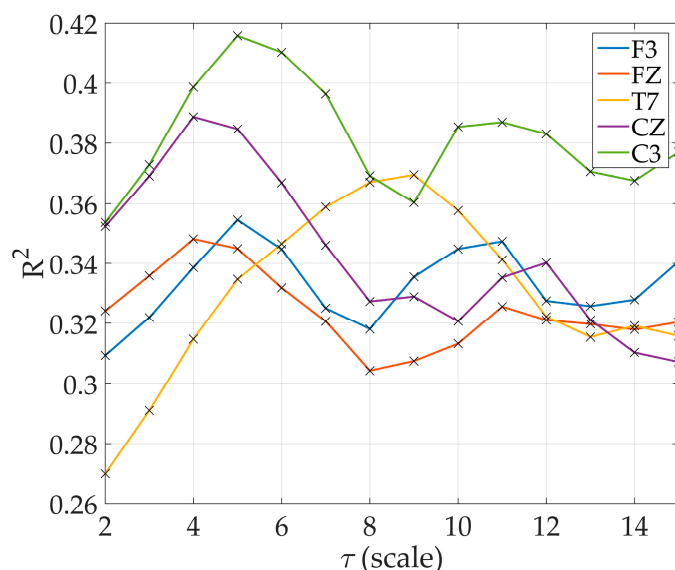


Figure 5. R^2 of regression models at electrode sites with MsE modified, at different scales, as main predictor.

In general, adding the squared term of the EEG marker did not produce a better model. Thus, the results of quadratic models were not specified in Tables 2 and 3. The scatterplot figures and regression line shown in Figures 3 and 4 describing the relationship of qEEG markers to the MMSE scores based on the regression model. Age, duration of illness, and years of education were set at their mean value shown in Table 1.

4. Discussion

There were 79 subjects diagnosed with probable AD who participated in this study. EEG recordings were taken while the subjects were sitting in an upright position in a resting state with their eyes closed. MMSE scores and demographic information such as age, duration of illness, and years of education were taken during assessment. The EEG recordings were visually selected before computation of the qEEG markers to remove irregular segments due to detached or loose electrodes. Cardiac and eye activities were automatically removed from the EEG. Forty 4-s epochs were selected from each patient. Calculation of the qEEG marker was derived from the mean value of 40 epochs per patient. The variance over the 40 epochs was computed for each marker to check stability. Linear regression models were calculated with MMSE as the dependent variable and the qEEG marker as the main independent variable. Age, duration of illness, and years of education served as the other independent variables to consider their effect on the MMSE scores. Regression models were computed at every electrode site for all qEEG markers. The significance of model was assessed by the Holm-Bonferroni method.

The results showed that the disease severity of probable AD, quantified by the MMSE scores of mild to moderate, was associated with the nonlinear qEEG markers of entropy and AMI. Regression models predicting MMSE with TsE or ShE as the main predictor variable achieved the highest R^2 at the electrodes T7 and F7, both positioned at the left side of the brain. This can be related to the study done by Ferreira et al. [28], where temporal lobe entropy was found to be a biomarker for conversion of mild cognitive impairment to AD due to atrophy of the left hippocampus and parahippocampal campus. For models with SpE as the main predictor, significant results were observed at C3 and T7. While a previous study on SpE of EEG signals between AD patients and normal controls did not produce significant differences [29], our results, however, showed an association with SpE to greater severity in probable AD patients. It's important to note, however, that the variance for the SpE markers were considerably higher than the other markers considered in this study. A reduction in complexity was seen with higher disease severity in SpE, MsE, and AMI. This loss of complexity was previously investigated in [9,10]. Our results showed increased ShE and TsE to greater disease severity. However, this does not automatically refute the common findings of reduced complexity in AD compared to normal controls. Since there were no normal controls in this study, no direct comparison between the AD and normal group was made. MsE modified returned significant regression models at almost all electrode sites of the brain from $\tau = 2$ where R^2 of 0.42 peaked at $\tau = 5$ for C3, and at scale $\tau = 10$ significant regression models across all electrodes were observed.

With AMI as the main predictor variable, though all electrode sites (except for T7 and T8) and clusters in the brain returned significant models, the electrode sites C3, Cz, and F3, as well as the central and left regions of the brain achieved the highest R^2 values (see Figure 4d). Jeong et al. [9] saw a correlation with the rate of decrease of AMI in the frontal and temporal regions while our results of models with AMI achieved the highest R^2 in the left and central region particularly at the sites C3, F3, and Cz (Figure 4d). Furthermore, MMSE also describes the 'global cognition' of a patient and as seen in the result, the AMI results across the all regions returned significant regression models. In comparison to the entropy markers where good results are concentrated at only certain electrode sites, AMI appeared to be able to describe the decline in global cognition of probable AD patients as seen in Table 2 and Figure 4. In comparison to the study of [14] where data from 64 patients were included, AMI R^2 remained high even with the addition of 15 patients. The same trend of increasing AMI with decreasing MMSE was also observed implying better predictability or reduced complexity as the disease worsens. With the new results, this paper strengthens the claim for AMI as a potential qEEG marker in the study of AD.

Studies linking disease severity of AD to other markers instead of qEEG markers were carried out such as [30] where (1) H-NMR spectroscopy resonances in the cerebrospinal fluid were found to be correlated with MMSE scores in AD patients. Benedictus et al. [31] found that lower cerebral blood flow (CBF) in the posterior brain region could be a marker for the rate of cognitive decline in AD where the decline was measured by the MMSE.

The strong points of our paper are the following: 79 patients with probable AD is the largest study compared to other similar papers [9,11–15] that dealt with complexity markers and AD. Furthermore, previous papers [9,11–13] that studied qEEG markers and AD patients involved comparing AD patients with normal controls or other dementia-related diseases such as MCI while this study focused on qEEG markers and AD patients with varying disease severity. While previous studies investigated SpE and dementia, this is the first time that SpE was analyzed together with disease severity of dementia patients with probable AD diagnosis.

The aim of this study was to investigate the potential of EEG entropy features in the diagnostic support of Alzheimer's diseases. The regression models with the most significant results based on R^2 were concentrated at the T7 and C3 electrode sites, and it would be interesting to carry out further investigations on this area. The effects of age and education on MMSE were verified by our results as they, as well as the duration of illness, were significant co-predictors in the regression models. AMI proved to be most closely related to disease severity, ranging from mild to moderate MMSE scores

based on the 79 patients, explaining up to 46% of the variation in the data. As seen in Figure 3, AMI increases with the decreasing MMSE. Given that higher AMI denotes better predictability, this suggests that less information processing and content is available in the EEG signal as the cognitive level of and probable AD patient declines. Next to AMI, MsE modified proved to be related to disease severity, explaining up to 42% of the variation in the data at scale $\tau = 5$ at C3. Therefore, we conclude that these quantitative EEG markers, AMI and MsE modified, should be investigated further in longitudinal studies to determine whether it can also aid in predicting AD progression.

Supplementary Materials: The following are available online at <https://www.dropbox.com/s/1ht2sez7u4lhafu/Supplementary.zip?dl=0>.

Acknowledgments: This study was supported by the Austrian Research Promotion Agency FFG under project No. 827462 and Dr. Grossger & DrBal GmbH, (Alpha Trace Medical Systems), Vienna.

Author Contributions: The qEEG study within PRODEM was initiated and designed by Heinrich Garn (H.G.) H.G. and Reinhold Schmidt (R.S.). Thomas Benke (T.B.), Peter Dal-Bianco (P.D.B.), Gerhard Ransmayr (G.R.), Stephan Seiler (S.S.), and R.S. performed the assessments of the patients and provided demographic and neuropsychological data. Manfred Deistler (M.D.) provided consultations in mathematics. Dieter Grossgger (D.G.) provided the EEG recording systems. Carmina Coronel (C.C.), Markus Waser (M.W.), and H.G. designed the investigation of the qEEG complexity markers. C.C. performed the computations and wrote the paper with H.G.

Conflicts of Interest: C.C., H.G., M.W., M.D., T.B., P.D.B., G.R., S.S., and R.S. declare no conflict of interest. D.G. is shareholder and managing director of the company that has provided the EEG measurement equipment that was used to collect the EEG data for this study.

Appendix A

The 79 patients in this study were all part of the prospective longitudinal studies of the Austrian Alzheimer Society (PRODEM). Written consent was given by the patients or their caregivers or family members. The patients were all diagnosed with AD probable according to the NINCDS-ADRDA criteria [4,17]. The NINCDS-ADRDA criteria require exclusion of other physical or neurological diseases that could have been responsible for the cognitive symptoms of a patient. MRI testing were considered in the diagnosis and probable AD was only diagnosed in the absence of infarctions in the territory of large vessels.

Appendix B

Cluster Name	Electrodes
anterior	Fp1, Fp2, Fp3, F4
anterior/temporal	Fp1, Fp2, F7, F3, F4, F8
central	Fz, C3, C4, Cz, Pz
posterior	P3, P4, O1, O2
posterior/temporal	P7, P3, P4, P8, O1, O2
temporal left	F7, T7, P7
temporal right	F8, T8, P8
left	Fp1, F3, F7, C3, T7, P3, P7, O1
right	Fp2, F4, F8, C4, T8, P4, P8, O2
all	Fp1, Fp2, F7, F3, Fz, F4, F8, T7, C3, Cz, C4, T8, P7, P3, Pz, P4, P8, O1, O2

References

1. Alzheimer's Association. 2016 Alzheimer's disease Facts and Figures. *Alzheimer Dement.* **2016**, *12*, 459–509.
2. Prince, M.; Wimo, A.; Guerchet, M.; Ali, G.C.; Wu, Y.T.; Prina, M. *World Alzheimer Report 2015*; Alzheimer's Disease International (ADI): London, UK, 2015.
3. Braak, H.; Rüb, U.; Schultz, C.; Del Tredici, K. Vulnerability of cortical neurons to Alzheimer's and Parkinson's diseases. *J. Alzheimer Dis.* **2006**, *9* (Suppl. 3), 35–44.

4. McKhann, G.; Drachman, D.; Folstein, M.; Katzman, R.; Price, D.; Stadlan, E.M. Clinical Diagnosis of Alzheimer's disease: Report of the NINCDS-ADRDA Work Group under the auspices of Department of Health and Human Services Task Force on Alzheimer's Disease. *Neurology* **1984**, *34*, 939. [[CrossRef](#)] [[PubMed](#)]
5. Johnson, K.A.; Fox, N.C.; Sperling, R.A.; Klunk, W.E. Brain Imaging in Alzheimer Disease. *Cold Spring Harb. Perspect. Med.* **2012**, *2*, a006213. [[CrossRef](#)] [[PubMed](#)]
6. Jackson, C.E.; Snyder, P.J. Electroencephalography and event-related potentials as biomarkers of mild cognitive impairment and mild Alzheimer's diseases. *Alzheimer Dement.* **2008**, *4* (Suppl. 1), S137–S143. [[CrossRef](#)] [[PubMed](#)]
7. Jeong, J. EEG dynamics in patients with Alzheimer's disease. *Clin. Neurophysiol.* **2004**, *115*, 1490–1505. [[CrossRef](#)] [[PubMed](#)]
8. Dauwels, J.; Vialatte, F.; Cichocki, A. Diagnosis of Alzheimer's Diseases from EEG Signals: Where Are We Standing? *Curr. Alzheimer Res.* **2010**, *7*, 487–505. [[CrossRef](#)] [[PubMed](#)]
9. Jeong, J.; Gore, J.C.; Peterson, B.S. Mutual information analysis of the EEG in patients with Alzheimer's disease. *Clin. Neurophysiol.* **2001**, *112*, 827–835. [[CrossRef](#)]
10. Yang, A.C.; Wang, S.J.; Lai, K.L.; Tsai, C.F.; Yang, C.H.; Hwang, J.P.; Lo, M.T.; Huang, N.E.; Peng, C.K.; Fuh, J.L. Cognitive and neuropsychiatric correlates of EEG dynamic complexity in patients with Alzheimer's disease. *Prog. Neuro-Psychopharmacol. Biol. Psychiatry* **2013**, *47*, 52–61. [[CrossRef](#)] [[PubMed](#)]
11. Escudero, J.; Abásolo, D.; Hornero, R.; Espino, P.; López, M. Analysis of electroencephalograms in Alzheimer's disease patients with multiscale entropy. *Physiol. Meas.* **2006**, *27*, 1091–1106. [[CrossRef](#)] [[PubMed](#)]
12. Mizuno, T.; Takashai, T.; Cho, R.Y.; Kikuchi, M.; Murata, T.; Takahashi, K.; Wada, Y. Assessment of EEG dynamical complexity in Alzheimer's disease using multiscale entropy. *Clin. Neurophysiol.* **2010**, *121*, 1438–1446. [[CrossRef](#)] [[PubMed](#)]
13. McBride, J.C.; Zhao, X.; Munro, N.B.; Smith, C.D.; Jicha, G.A.; Hively, L.S.; Broster, L.S.; Schmitt, F.A.; Kruscio, R.J.; Jiang, Y. Spectral and Complexity Analysis of Scalp EEG Characteristics for Mild Cognitive Impairment and Early Alzheimer's Disease. *Comput. Methods Programs Biomed.* **2014**, *114*, 153–163. [[CrossRef](#)] [[PubMed](#)]
14. Garn, H.; Waser, M.; Deistler, M.; Benke, T.; Dal-Bianco, P.; Ransmayr, G.; Schmidt, H.; Sanin, G.; Santer, P.; Caravias, G.; et al. Electroencephalographic Complexity Markers Explain Neuropsychological Test Scores in Alzheimer's Disease. In Proceedings of the 2014 IEEE-EMBS International Conference on Biomedical and Health Informatics, Valencia, Spain, 1–4 June 2014.
15. Garn, H.; Waser, M.; Deistler, M.; Benke, T.; Dal-Bianco, P.; Ransmayr, G.; Schmidt, H.; Sanin, G.; Santer, P.; Caravias, G.; et al. Quantitative EEG markers relate to Alzheimer's diseases severity in the Prospective Dementia Registry Austria (PRODEM). *Clin. Neurophysiol.* **2015**, *126*, 505–513. [[CrossRef](#)] [[PubMed](#)]
16. Folstein, M.F.; Folstein, S.E.; McHugh, P.R. Mini-Mental State. A Practical Method for grading the cognitive state of patients for the clinician. *J. Psychiatr. Res.* **1975**, *12*, 189–198. [[CrossRef](#)]
17. Dubois, B.; Feldman, H.H.; Jacova, C.; Dekosky, S.T.; Barberger-Gateau, P.; Cummings, J.; Delacourte, A.; Galasko, D.; Gauthier, S.; Jicha, G.; et al. Research Criteria for the diagnosis of Alzheimer's disease: Revising the NINCDS-ADRDA criteria. *Lancet Neurol.* **2007**, *6*, 734–746. [[CrossRef](#)]
18. Waser, M.; Garn, H. Removing cardiac interference from the electroencephalogram using a modified Pan-Tompkins algorithm and linear regression. Engineering in Medicine and Biology Society (EMBC). In Proceedings of the 2013 35th Annual International Conference of the IEEE, Osaka, Japan, 3–7 July 2013; pp. 2028–2031.
19. Draper, N.R.; Smith, H. *Applied Regression Analysis*, 3rd ed.; John Wiley and Sons Inc.: New York, NY, USA, 1988.
20. Kaplan, A.Y.; Fingelkurt, A.A.; Fingelkurt, A.A.; Borisov, S.V.; Barkhovsky, B.S. Nonstationary nature of the brain activity as revealed by EEG/MEG: Methodological, practical and conceptual challenges. *Signal Process.* **2005**, *85*, 2190–2212. [[CrossRef](#)]
21. Dickey, D.A.; Fuller, W.A. Distribution of the estimators for autoregressive time series with a unit root. *J. Am. Stat. Assoc.* **1979**, *74*, 427–431. [[CrossRef](#)]
22. Rezek, A.; Roberts, S.J. Stochastic complexity markers for physiological signal analysis. *IEEE Trans. Biomed. Eng.* **1998**, *45*, 1186–1191. [[CrossRef](#)] [[PubMed](#)]

23. Costa, M.; Goldberger, A.L.; Peng, C.K. Multiscale entropy analysis of biological signals. *Phys. Rev. E Stat. Nonlinear Soft Matter Phys.* **2005**, *71 Pt 1*, 021906. [[CrossRef](#)] [[PubMed](#)]
24. Wu, S.D.; Wu, C.W.; Lee, K.Y.; Lin, S.G. Modified multiscale entropy for short-term time series analysis. *Phys. A Stat. Methods Appl.* **2013**, *392*, 5865–5873. [[CrossRef](#)]
25. Cover, T.M.; Thomas, J.A. *Elements of Information Theory*; Wiley: New York, NY, USA, 1991.
26. Tombaugh, T.N.; McIntyre, N.J. The mini-mental state examination: A comprehensive review. *J. Am. Geriatr. Soc.* **1992**, *40*, 922–935. [[CrossRef](#)] [[PubMed](#)]
27. Holm, S. A simple sequentially rejective multiple test procedure. *Scand. J. Stat.* **1979**, *6*, 65–70.
28. Ferreira, L.K.; Diniz, B.S.; Forlenza, O.V.; Busatto, G.F.; Zanetti, M.V. Neurostructural predictors of Alzheimer's disease: A meta-analysis of VBM studies. *Neurobiol. Aging* **2011**, *32*, 1733–1741. [[CrossRef](#)] [[PubMed](#)]
29. Abásolo, D.; Hornero, R.; Espino, P.; Álvarez, D.; Poza, J. Entropy analysis of the EEG background activity in Alzheimer's disease patients. *Physiol. Meas.* **2006**, *27*, 241–253. [[CrossRef](#)] [[PubMed](#)]
30. Kork, F.; Gentsch, A.; Holthues, J.; Hellweg, R.; Jankowski, V.; Tepel, M.; Zidek, W.; Jankowski, J. A biomarker for severity of Alzheimer's disease: ^1H -NMR resonances in cerebrospinal fluid correlate with performance in mini-mental-state-exam. *Biomarkers* **2012**, *17*, 36–42. [[CrossRef](#)] [[PubMed](#)]
31. Benedictus, M.R.; Leeuwis, A.E.; Binnewijzend, M.A.A.; Kuijer, J.P.A.; Scheltens, P.; Barkhof, F.; van der Flier, W.M.; Prins, N.D. Lower cerebral blood flow is associated with faster cognitive decline in Alzheimer's disease. *Eur. Radiol.* **2016**. [[CrossRef](#)] [[PubMed](#)]



© 2017 by the authors. Licensee MDPI, Basel, Switzerland. This article is an open access article distributed under the terms and conditions of the Creative Commons Attribution (CC BY) license (<http://creativecommons.org/licenses/by/4.0/>).